ATTITUDE MODE ESTIMATION FROM COMPUTER VISION DATA VIA MULTIPLE MODEL METHODS

Scott Geyer and John L. Crassidis

**The Research Foundation for SUNY
on behalf of University at Buffalo
The UB Commons
520 Lee Entrance, Suite 211
Amherst, NY 14228-2567**

18 December 2019

Final Report

APPROVED FOR PUBLIC RELEASE; DISTRIBUTION IS UNLIMITED.

AIR FORCE RESEARCH LABORATORY
Space Vehicles Directorate
3550 Aberdeen Ave SE
AIR FORCE MATERIEL COMMAND
KIRTLAND AIR FORCE BASE, NM 87117-5776

NOTICE AND SIGNATURE PAGE

Using Government drawings, specifications, or other data included in this document for any purpose other than Government procurement does not in any way obligate the U.S. Government. The fact that the Government formulated or supplied the drawings, specifications, or other data does not license the holder or any other person or corporation; or convey any rights or permission to manufacture, use, or sell any patented invention that may relate to them.

This report is the result of contracted fundamental research which is exempt from public affairs security and policy review in accordance with AFI 61-201, paragraph 2.3.5.1. This report is available to the general public, including foreign nationals. Copies may be obtained from the Defense Technical Information Center (DTIC) (http://www.dtic.mil).

AFRL-RV-PS-TR-2019-00141 HAS BEEN REVIEWED AND IS APPROVED FOR PUBLICATION IN ACCORDANCE WITH ASSIGNED DISTRIBUTION STATEMENT.

//SIGNED//

//SIGNED//

_____

_____

THOMAS LOVELL
Program Manager

DAVID WILT
Tech Advisor, Space Component Technology
Branch (Acting)

//SIGNED//

_____

JOHN BEAUCHEMIN
Chief Engineer, Spacecraft Technology Division
Space Vehicles Directorate

This report is published in the interest of scientific and technical information exchange, and its publication does not constitute the Government's approval or disapproval of its ideas or findings.

REPORT DOCUMENTATION PAGE

The public reporting burden for this collection of information is estimated to average 1 hour per response, including the time for reviewing instructions, searching existing data sources, gathering and maintaining the data needed, and completing and reviewing the collection of information. Send comments regarding this burden estimate or any other aspect of this collection of information, including suggestions for reducing the burden, to Department of Defense, Washington Headquarters Services, Directorate for Information Operations and Reports (0704-0188), 1215 Jefferson Davis Highway, Suite 1204, Arlington, VA 22202-4302. Respondents should be aware that notwithstanding any other provision of law, no person shall be subject to any penalty for failing to comply with a collection of information if it does not display a currently valid OMB control number.
PLEASE DO NOT RETURN YOUR FORM TO THE ABOVE ADDRESS.

1. REPORT DATE (DD-MM-YYYY)	2. REPORT TYPE	3. DATES COVERED (From - To)
18-Dec-2019	Final Report	22-Dec-2017 to 18-Dec-2019

4. TITLE AND SUBTITLE

Attitude Mode Estimation from Computer Vision Data via Multiple Model Methods

5a. CONTRACT NUMBER

FA9453-18-1-0008

5b. GRANT NUMBER

5c. PROGRAM ELEMENT NUMBER

62601F

6. AUTHOR(S)

Scott Geyer and John Crassidis

5d. PROJECT NUMBER

8809

5e. TASK NUMBER

EF130345

5f. WORK UNIT NUMBER

V182

7. PERFORMING ORGANIZATION NAME(S) AND ADDRESS(ES)

The Research Foundation for SUNY on behalf of University at Buffalo
The UB Commons
520 Lee Entrance, Suite 211
Amherst, NY 14228-2567

8. PERFORMING ORGANIZATION REPORT NUMBER

9. SPONSORING/MONITORING AGENCY NAME(S) AND ADDRESS(ES)

Air Force Research Laboratory
Space Vehicles Directorate
3550 Aberdeen Ave., SE
Kirtland AFB, NM 87117-5776

10. SPONSOR/MONITOR'S ACRONYM(S)

AFRL/RVSV

11. SPONSOR/MONITOR'S REPORT NUMBER(S)

AFRL-RV-PS-TR-2019-0141

12. DISTRIBUTION/AVAILABILITY STATEMENT

Approved for public release; distribution is unlimited

13. SUPPLEMENTARY NOTES

14. ABSTRACT

This report outlines the finished result in the scope of the work, which is Pointing Mode Determination of Resident Space Objects (RSOs). RSOs are any object orbiting another body, but this work focuses on selective satellites of which little information is known. The goal is to improve Space Situational Awareness (SSA) to be able to determine the intent of the spacecraft, as well as provide any other useful information. This information can be gathered using algorithms with information from resolved images of the RSO. The resolved images can be obtained with an Observing Satellite (OS), which is tasked with staying close to and pointing its sensor in the direction of the RSO. For the purposes of this work, the OS is already in place, orbiting near the RSO with a controller keeping the OS pointing at the RSO, and is taking resolved images. The input to the provided work is in the form of already-extracted feature points of the RSO in a two-dimensional image plane, used as measurements for the attitude determination algorithms of the Extended Kalman Filter.

15. SUBJECT TERMS

Space Situational Awareness, Pointing Mode Determination, Resident Space Objects, Assess Patterns of Life, Computer Vision Data, Mulitple-Model Adaptive

16. SECURITY CLASSIFICATION OF:			17. LIMITATION OF ABSTRACT	18. NUMBER OF PAGES	19a. NAME OF RESPONSIBLE PERSON
a. REPORT	b. ABSTRACT	c. THIS PAGE			Thomas Lovell
U	U	U	SAR	30	19b. TELEPHONE NUMBER (Include area code)

--- **This Page Intentionally Left Blank** ---

Table of Contents

List of Figures

List of Tables

1.0   SUMMARY

This report outlines the finished result in the scope of the work, which is Pointing Mode Determination of Resident Space Objects (RSOs). RSOs are any object orbiting another body, but this work focuses on selective satellites of which little information is known. The goal is to improve Space Situational Awareness (SSA) to be able to determine the intent of the spacecraft, as well as provide any other useful information. This information can be gathered using algorithms with information from resolved images of the RSO. The resolved images can be obtained with an Observing Satellite (OS). For the purposes of this work, the OS is already in place, orbiting near the RSO with a controller keeping the OS pointing at the RSO, and is taking resolved images. The input to the provided work is in the form of already-extracted feature points of the RSO in a two-dimensional image plane, used as measurements for the attitude determination algorithms of the Extended Kalman Filter (EKF).

Any object in space can pose a threat, and one step in improving SSA and assessing the threat of an RSO is determining the attitude mode of the RSO, such as Sun-pointing, Earth-pointing, uncontrolled tumble, etc. One proposed method of doing this is to track prominent features of the RSO and compare their trajectories to would-be trajectories of the same features given certain control laws specified by a multiple model adaptive estimator (MMAE). The MMAE uses a bank of EKFs, each utilizing a different control law, and probabilistically compares the output of each control law with what is seen in the measurements. The control law acts to change the orientation of the object in the preferred manner, and each attitude mode will utilize a control law to keep the object pointing in the preferred direction, if there is one. Therefore, control laws are indicative of the attitude mode of the object, and so determining which control law the object is following will subsequently determine the attitude mode. The EKFs in the MMAE require measurements of the locations of the features of the target RSO, and these measurements come from a sensor on the OS. The measurements alone do not give enough information about the RSO to determine its attitude mode without implementing the dynamics of the system. The dynamics of the OS relative to the target RSO is modeled as formation flying, with the full dynamics of the two satellites modeled in the Hill Frame, which is attached to the RSO at all times while it orbits the Earth. With the relative position of the two satellites being estimated, the OS is also given a control law which works to keep the RSO in the center of the image plane. With this assumption, attitude dynamics as well as orbital dynamics will be coupled in the MMAE to estimate the quaternions of both the RSO and OS as well as their relative positions. The information of the quaternions at each time step are then used to compare a set of RSO control laws to what is observed in order to determine the correct attitude mode.

2.0 INTRODUCTION

Space situational awareness (SSA) is described as having the knowledge and information of resident space objects (RSOs). This information could range from knowledge of attitude modes, maneuvers, and orbits to reasonable predictions of actions which can be taken by the RSO. All of this information requires having knowledge of the attitude of the RSO. Resolved images of the target can be obtained with a sensor attached to an observing satellite (OS), so long as the OS stays close to the target RSO. The resolved images are coupled with object detection algorithms to be able to pick out prominent features on the object, and the features are tracked to give measurements as locations of the features on the RSO as they appear in the image. This information alone is not enough to be able to determine the attitude mode of the RSO, so the attitude determination Multiple Model Adaptive Estimator (MMAE) algorithm is implemented with the tracked feature points as measurements.

The location of measurements in a set of images can be converted to useful information if the position of the RSO and the OS are known. Since the OS needs to be close to the RSO in order to take resolved images, formation flying dynamics can be used to describe the relationship between the two spacecraft. The formation flying dynamics will be implemented in Extended Kalman Filters (EKFs) such that the attitude and position of the RSO are estimated. Once this information is obtained, control laws can be used to determine how the RSO would act given different attitude mode settings. The MMAE will compare several different control laws with the observed movements of the RSO, and the probability of each attitude mode being the one used by the RSO will be obtained. [1] When the probability of one mode is large enough, it can be reasonably determined what attitude mode the RSO is using, thus determining the pointing mode and increasing SSA.

3.0   PROBLEM SETUP

3.1   Defining the Problem

The RSO and OS are in a formation flying scenario, which is modeled in the Hill Frame. The Hill Frame moves with the RSO, with the $\hat{\mathbf{o}}_{\mathbf{r}}$ direction pointing radially outward from the Earth through the satellite. The $\hat{\mathbf{o}}_{\mathbf{h}}$ direction points in line with the angular momentum vector of the RSO orbit, and the $\hat{\mathbf{o}}_\theta$ direction finishes the triad. The Hill Frame is demonstrated in Figure 1, where the RSO is modeled as the chief and the OS is modeled as the deputy in this scenario.
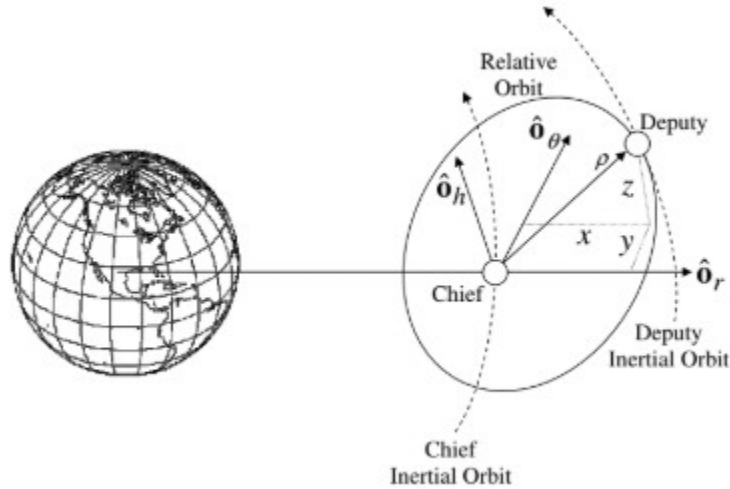
Figure 1: The relationship of RSO and OS in a formation flying scenario

The unknown position vector from the RSO to the OS is $\rho_c = \begin{bmatrix} x & y & z \end{bmatrix}^T$, expressed in the Hill Frame. The prominent features of the RSO are known locations with respect to the RSO body frame, shown in Figure 2 as V_i, and the vector from the OS to the prominent features is $V_i - \rho_c$. This vector, when used in the correct form, can be used to show where the prominent features appear in the OS images, but the locations of the prominent features need to be expressed in its body frame in order to be useful, which is shown as

$$b_i =^D A^C V_i + \rho_d \tag{1}$$

$$i = 1, 2, ..., N$$

Where N is the number of feature points on the RSO, ρ_d is the position vector from the

OS to the RSO, and $^D A^C$ is the relative attitude matrix between the RSO and the OS. A controller will be used to point the sensor of the OS in the direction of the RSO, and this controller will be given an initial condition for the attitude and then will have constrained movements to keep the sensor pointed at the RSO without performing extensive maneuvers. The initial condition is a reference attitude for the OS to convert from the Hill Frame to its Body Frame given by

$$^D A^H = \begin{bmatrix} \frac{y\dot{z}-z\dot{y}}{\|\rho_c \times \dot{\rho}_c\|} & \frac{z\dot{x}-x\dot{z}}{\|\rho_c \times \dot{\rho}_c\|} & \frac{x\dot{y}-y\dot{x}}{\|\rho_c \times \dot{\rho}_c\|} \\ a_{32}a_{13}-a_{33}a_{12} & a_{33}a_{11}-a_{31}a_{13} & a_{31}a_{12}-a_{32}a_{11} \\ \frac{-x}{\|\rho_c\|} & \frac{-y}{\|\rho_c\|} & \frac{-z}{\|\rho_c\|} \end{bmatrix} \tag{2}$$

where the a_{ij} terms refer to the terms within its own matrix. This reference attitude matrix is chosen because it points the sensor, which is along the $\hat{z}_d$ direction of the OS, directly at the RSO, and it also starts the controller with the $\hat{x}_d$ vector along the direction of the relative angular momentum. Once the initial reference attitude is determined, the subsequent reference attitudes are found by merging the previous attitude with the new estimates. Figure 2 gives a rough idea of the orientation of each satellite within the Hill Frame.
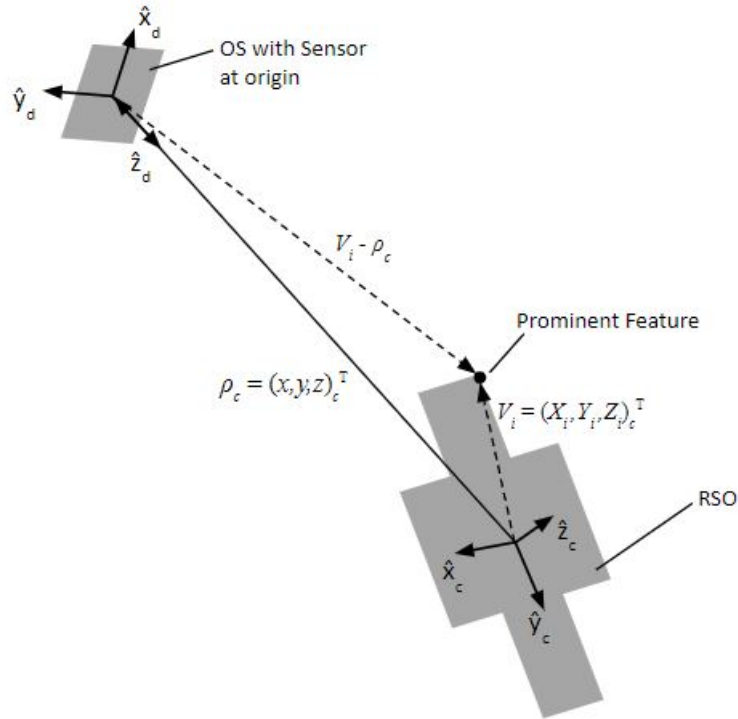
Figure 2: The vectors of association between RSO and OS

The attitude matrix in Equation (2) is required to have information about the relative position of the two satellites to complete the reference attitude. The orbit of the RSO is found via orbit determination algorithms, which is out of scope of this project. The position of the

OS with respect to the RSO is estimated in the following chapters, and can be implemented into the reference attitude from there.

3.2 Creating Measurements

In the field, the sensor on the OS will take images and track the feature points of the RSO, and the measurements will be the locations of the feature points as they appear in the images. For the purposes of creating an attitude determination and pointing mode estimator, measurements must be simulated. A brief overview of how that is done is shown here.

An orbit must be picked for the RSO to base the relative dynamics off of. A geosynchronous orbit is chosen, with the only requirement of any orbital element to meet this orbit being the semimajor axis. Each of the other orbital elements, being the eccentricity, initial true anomaly, inclination angle, right ascension angle, and argument of periapsis are each chosen arbitrarily. The equation used to find the semimajor axis, a, to meet the demands of a geosynchronous orbit is

$$P^2 = \frac{4\pi^2 a^3}{G(M+m)} \tag{3}$$

where P is the orbital period of one day, G is the gravitational constant, M is the mass of the Earth and m is the mass of the RSO, which can be ignored. From the orbital elements, the initial position and velocity of the RSO can be derived, and the orbital equation is used to propagate the orbit

$$\ddot{\boldsymbol{r}} = -\frac{\mu}{r^3}\boldsymbol{r} \tag{4}$$

where $\boldsymbol{r}$ is the vector of the position of the satellite, $\mu = GM$, and $r = \|\boldsymbol{r}\|$.

The project is set up such that the OS is 'close' to the RSO, so other than that requirement its orbit is also somewhat arbitrary. The orbit for the OS is picked such that the positional elements, being the eccentricity, semimajor axis, and initial true anomaly, are the same as the RSO, and the orientational elements, being the inclination angle, right ascension angle, and argument of periapsis, are changed slightly so that the OS stays within roughly 1km of the RSO. The picked orbital elements are then used to solve for the initial conditions of the orbit, and the relative orbital equations are used to propagate the relative position of the OS and RSO in the Hill Frame. [2]

$$\ddot{x} - x\dot{\theta}^2 \left(1 + 2\frac{r_c}{p}\right) - 2\dot{\theta}\left(\dot{y} - y\frac{\dot{r}_c}{r_c}\right) = 0 \tag{5a}$$

$$\ddot{y} + 2\dot{\theta}\left(\dot{x} - x\frac{\dot{r}_c}{r_c}\right) - y\dot{\theta}^2\left(1 - \frac{r_c}{p}\right) = 0 \tag{5b}$$

$$\ddot{z} + z\dot{\theta}^2\frac{r_c}{p} = 0 \tag{5c}$$

$$\ddot{\theta} = -2\frac{\dot{r}_c}{r_c}\dot{\theta} \tag{5d}$$

$$\ddot{r}_c = r_c\dot{\theta}^2\left(1 - \frac{r_c}{p}\right) \tag{5e}$$

Where p is the semilatus rectum of the RSO orbit, r_c is the radius of the RSO orbit wrt the Earth, and θ is the true anomaly of the RSO.

In building the scenario for the mode estimation algorithm, Equation 5 determines the orbital positions of the two spacecraft. The OS attitude controller uses a reference attitude which is determined by some of the states from Equation 5 and some of the estimates in the filter, which is discussed later. The final piece of the scenario before the filter can be constructed is the RSO attitude. The RSO acts independently of the OS in its attitude dynamics, but the scenario being built will test the estimator for each of the possible modes. The modes being considered are Sun Pointing, Earth Pointing, Inertial Pointing, and Uncontrolled Tumble. The simulation is allowed to run for three orbital periods, and Table 1 shows the sequence of modes controlling the RSO.

Table 1: RSO Controller Mode Schedule

Time [s]	Mode
1−64799	1
64800−129599	2
129600−194399	0
194400−259200	3

Now, the orientation and relative position of each satellite has been built for the use scenario. Using Equation (1), the vector from the OS to each of the feature points on the RSO is known. The colinearity equations are used to then obtain the location of each feature point as they would appear in the images from the OS according to the reference frames shown in Figure 2.

$$\alpha = -f\frac{b_{2,i}}{b_{3,i}} \quad \beta = -f\frac{b_{1,i}}{b_{3,i}} \tag{6}$$

$$i = 1, 2, ..., N$$

where f is the focal length of the OS sensor. α and β are used as the measurements when creating the attitude and pointing mode estimator.

4.0 EXTENDED KALMAN FILTER

With the measurements coming in from the OS, an Extended Kalman Filter (EKF) is used to estimate both the relative position of the two satellites as well as each satellite's attitude relative to the Hill Frame.[3] A derivation of the equations of the EKF can be found in [4].

The EKF states that the OS and RSO will each have an angular rate measurement from a rate integrating gyro, and each gyro will have a bias. This will be the case for the OS, but little is known about the RSO and there will not be angular rate measurements supplied from it. Instead, the filter will assume that the RSO is set to a specific mode, and it will model the RSO controller and propagation from the estimate rather than with gyro measurement information.

4.1 Kalman Gain

The EKF is initialized with initial relative quaternion estimates between the RSO and Hill Frame, $\hat{q}_{c/H}$, and the OS and Hill Frame, $\hat{q}_{d/H}$, the drift for both OS and RSO, $\hat{\beta}$, relative position and its rate of change $\hat{\rho}$ and $\hat{\dot{\rho}}$, radius of RSO orbit and its rate of change, $\hat{r}_c$ and $\hat{\dot{r}}_c$, the true anomaly and its rate of change, $\hat{\theta}$ and $\hat{\dot{\theta}}$, and the state covariance, P.

$$\hat{q}_{c/H}(t_0) = q_{\hat{c}/H} \quad \hat{q}_{d/H}(t_0) = q_{\hat{d}/H} \quad \hat{\beta}_c(t_0) = \hat{\beta}_{c_0} \quad \hat{\beta}_d(t_0) = \hat{\beta}_{d_0} \quad \hat{\rho}(t_0) = \hat{\rho}_0 \quad \hat{\dot{\rho}}(t_0) = \hat{\dot{\rho}}_0$$

$$\hat{r}_c(t_0) = \hat{r}_{c_0} \quad \hat{\dot{r}}_c(t_0) = \hat{\dot{r}}_{c_0} \quad \hat{\theta}(t_0) = \hat{\theta}_0 \quad \hat{\dot{\theta}}(t_0) = \hat{\dot{\theta}}_0 \quad P(t_0) = P_0$$

The Kalman Gain is calculated with the equation

$$K_k = P_k^- H_k^T(\hat{q}_k^-) \left[H_k^T(\hat{q}_k^-) P_k^- H_k^T(\hat{q}_k^-) + R_k \right]^{-1} \tag{7}$$

with the parameters in the Kalman Gain equation defined as the following series of equations. [3] [4]

$$H_k(\hat{x}_k^-) = \begin{bmatrix} \left[A_H^d(\hat{q}_{d/H}^-)\hat{r}_1^- \times \right] & \frac{\partial \hat{b}_1^-}{\partial \delta\alpha_{c/H}} & 0_{3\times 6} & \frac{\partial \hat{b}_1^-}{\partial \hat{\rho}^-} & 0_{3\times 7} \\ \vdots & \vdots & \vdots & \vdots & \vdots \\ \left[A_H^d(\hat{q}_{d/H}^-)\hat{r}_N^- \times \right] & \frac{\partial \hat{b}_N^-}{\partial \delta\alpha_{c/H}} & 0_{3\times 6} & \frac{\partial \hat{b}_N^-}{\partial \hat{\rho}^-} & 0_{3\times 7} \end{bmatrix} \tag{8a}$$

$$A(q) = \Xi^T(q)\Psi(q) = \begin{bmatrix} q_4 I_{3\times 3} + [\varrho\times] \\ -\varrho^T \end{bmatrix} \begin{bmatrix} q_4 I_{3\times 3} - [\varrho\times] \\ -\varrho^T \end{bmatrix} \tag{8b}$$

$$r_i = \frac{V_i - \hat{\rho}}{\|V_i - \hat{\rho}\|} \tag{8c}$$

$$\frac{\partial \hat{b}_i^-}{\partial \delta \alpha_{c/H}} = A_H^d(\hat{q}_{d/H}^-) \frac{\partial \hat{r}_i^-}{\partial \hat{\rho}^-} \left[A_H^c(\hat{q}_{c/H}^-) \right]^T [V_i \times] \tag{8d}$$

$$\frac{\partial \hat{b}_i^-}{\partial \hat{\rho}^-} = A(\hat{q}^-) \frac{\partial \hat{r}_i^-}{\partial \hat{\rho}^-} \tag{8e}$$

$$\frac{\partial \hat{r}_i^-}{\partial \hat{\rho}^-} = \frac{1}{\hat{s}_i^-} \begin{bmatrix} -[(Y_i - \hat{y}^-)^2 + (Z_i - \hat{z}^-)^2] & (X_i - \hat{x}^-)(Y_i - \hat{y}^-) & (X_i - \hat{x}^-)(Z_i - \hat{z}^-) \\ (X_i - \hat{x}^-)(Y_i - \hat{y}^-) & -[(X_i - \hat{x}^-)^2 + (Z_i - \hat{z}^-)^2] & (Y_i - \hat{y}^-)(Z_i - \hat{z}^-) \\ (X_i - \hat{x}^-)(Z_i - \hat{z}^-) & (Y_i - \hat{y}^-)(Z_i - \hat{z}^-) & -[(X_i - \hat{x}^-)^2 + (Y_i - \hat{y}^-)^2] \end{bmatrix} \tag{8f}$$

$$\hat{s}_i^- = \left[(X_i - \hat{x}^-)^2 + (Y_i - \hat{y}^-)^2 + (Z_i - \hat{z}^-)^2 \right]^{3/2} \tag{8g}$$

$$R_k = \begin{bmatrix} R_1 & 0 & 0 \\ 0 & \ddots & 0 \\ 0 & 0 & R_N \end{bmatrix} \tag{9a}$$

$$R_i = \mathfrak{R}_i + \frac{1}{2} trace(\mathfrak{R}_i) b_i b_i^T \tag{9b}$$

$$\mathfrak{R}_i = E v_i v_i^T = J_i R_i^{FOCAL} J_i^T \tag{9c}$$

$$J_i = \frac{1}{\sqrt{1 + \alpha_i^2 + \beta_i^2}} \begin{bmatrix} -1 & 0 \\ 0 & -1 \\ 0 & 0 \end{bmatrix} - \frac{1}{1 + \alpha_i^2 + \beta_i^2} b_i \begin{bmatrix} \alpha_i & \beta_i \end{bmatrix} \tag{9d}$$

$$b_i = \frac{1}{\sqrt{f^2 + \alpha_i^2 + \beta_i^2}} \begin{bmatrix} -\alpha_i \\ -\beta_i \\ f \end{bmatrix} \tag{9e}$$

$$R_i^{FOCAL} = \frac{\sigma_i^2}{1 + d(\alpha_i^2 + \beta_i^2)} \begin{bmatrix} (1 + d\alpha_i^2)^2 & (d\alpha_i \beta_i)^2 \\ (d\alpha_i \beta_i)^2 & (1 + d\beta_i^2)^2 \end{bmatrix} \tag{9f}$$

where d is a constant close to 1 and σ is the variance of measurement errors.

4.2 Update

With the Kalman Gain calculated, the EKF can move forward to the Update step. In this step, the measurement covariance as well as each of the propagated parameters are updated. These parameters include a small angle error correction of the relative quaternion estimates for both the RSO and OS, $\delta\alpha_{c/H}$ and $\delta\alpha_{d/H}$, corrections for the drift of both the OS and RSO, $\Delta\beta$, corrections for the relative position and position rate of change, $\Delta\rho$ and $\Delta\dot{\rho}$, corrections for the radius of the RSO orbit and its rate of change, Δr_c and $\Delta\dot{r}_c$, and corrections for the true anomaly and true anomaly rate of the RSO orbit, $\Delta\theta$ and $\Delta\dot{\theta}$. These correction terms are found using the Kalman gain and the residual between the measurement and the estimate vector.

$$\Delta\hat{x}_k^+ = K_k\nu \tag{10}$$

where

$$\Delta\hat{x}_k^+ = \begin{bmatrix} \delta\alpha_{d/H}^T & \delta\alpha_{c/H}^T & \Delta\beta_c^T & \Delta\beta_d^T & \Delta\rho^T & \Delta\dot{\rho}^T & \Delta r_c & \Delta\dot{r}_c & \Delta\theta_c & \Delta\dot{\theta}_c \end{bmatrix}$$

and

$$\nu = \tilde{y}_k - h_k(\hat{q}_{d/c}^-) \tag{11}$$

with

$$\tilde{y}_k = \begin{bmatrix} \tilde{b}_1^T & \tilde{b}_2^T & \cdots \tilde{b}_N^T \end{bmatrix}$$

and

$$h_k(\hat{q}_{d/c}^-) = \begin{bmatrix} A(\hat{q}_{d/c}^-)r_1 \\ A(\hat{q}_{d/c}^-)r_2 \\ \vdots \\ A(\hat{q}_{d/c}^-)r_N \end{bmatrix} \tag{12}$$

where

$$q_{d/c} = q_{d/H} \otimes q_{c/H}^{-1} \tag{13}$$

The corrections are implemented into the estimates through the following relations, which completes the Update section of the EKF.

$$\hat{q}_{c/H_k}^+ = \hat{q}_{c/H_k}^- + \frac{1}{2}\Xi(\hat{q}_{c/H_k}^-)\delta\alpha_{c/H}^T \tag{14a}$$

$$\hat{q}_{d/H_k}^+ = \hat{q}_{d/H_k}^- + \frac{1}{2}\Xi(\hat{q}_{d/H_k}^-)\delta\alpha_{d/H}^T \tag{14b}$$

$$\hat{\beta}_{c_k}^+ = \hat{\beta}_{c_k}^- + \Delta\hat{\beta}_{c_k}^+ \tag{14c}$$

$$\hat{\beta}_{d_k}^+ = \hat{\beta}_{d_k}^- + \Delta\hat{\beta}_{d_k}^+ \tag{14d}$$

9

$$\hat{\rho}^+ = \hat{\rho}^- + \Delta\rho \tag{14e}$$

$$\dot{\hat{\rho}}^+ = \dot{\hat{\rho}}^- + \Delta\dot{\rho} \tag{14f}$$

$$\hat{r}_c^+ = \hat{r}_c^- + \Delta r_c \tag{14g}$$

$$\dot{\hat{r}}_c^+ = \dot{\hat{r}}_c^- + \Delta\dot{r}_c \tag{14h}$$

$$\hat{\theta}^+ = \hat{\theta}^- + \Delta\theta \tag{14i}$$

$$\dot{\hat{\theta}}^+ = \dot{\hat{\theta}}^- + \Delta\dot{\theta} \tag{14j}$$

4.3   Propagation

The EKF propagates the estimates of the angular rates as well as the relative quaternions and covariance matrix using the discretized models of the system, which are derived in [4].

$$\hat{\omega}_{c_k}^+ - \hat{\beta}_{c_k}^+ \tag{15a}$$

$$\hat{\omega}_{d_k}^+ - \hat{\beta}_{d_k}^+ \tag{15b}$$

This completes the propagation of the angular rates based on the drift of the rate integrating gyros. The angular rates are then used to propagate the relative quaternions as follows.

$$\hat{q}_{d/H_{k+1}} = \bar{\Omega}(\hat{\omega}_{d/I_k}^d)\bar{\Gamma}(\hat{\omega}_{H/I_k}^H)\hat{q}_{d/H_k} \tag{16a}$$

where

$$\bar{\Omega}(\omega_{d/I_k}^d) = \begin{bmatrix} cos(\frac{1}{2}\left\|\omega_{d/I_k}^d\right\|\Delta t)I_{3\times3} - [\Psi_k\times] & \Psi_k \\ -\Psi_k^T & cos(\frac{1}{2}\left\|\omega_{d/I_k}^d\right\|\Delta t) \end{bmatrix} \tag{16b}$$

with

$$\Psi_k = \frac{sin(\frac{1}{2}\left\|\omega_{d/I_k}^d\right\|\Delta t)\omega_{d/I_k}^d}{\left\|\omega_{d/I_k}^d\right\|}$$

and

$$\bar{\Gamma}(\omega_{H/I_k}^H) = \begin{bmatrix} cos(\frac{1}{2}\left\|\omega_{H/I_k}^H\right\|\Delta t)I_{3\times3} - [\zeta_k\times] & -\zeta_k \\ \zeta_k^T & cos(\frac{1}{2}\left\|\omega_{H/I_k}^H\right\|\Delta t) \end{bmatrix} \tag{16c}$$

with

$$\zeta_k = \frac{sin(\frac{1}{2}\left\|\omega_{H/I_k}^H\right\|\Delta t)\omega_{H/I_k}^H}{\left\|\omega_{H/I_k}^H\right\|}$$

Using the same equation structures seen in Equation 15, $\hat{q}_{c/H_{k+1}}$ can be calculated by

$$\hat{q}_{c/H_{k+1}} = \bar{\Omega}(\hat{\omega}_{c/I_k}^d)\bar{\Gamma}(\hat{\omega}_{H/I_k}^H)\hat{q}_{c/H_k} \tag{17}$$

Where the RSO qauternion and angular rate is substituted in for the OS quaternion and angular rate from Equation 15. The State Covariance is also propagated with the following equations

$$P_{k+1}^- = \Phi_k P_k^+ \Phi_k^T + \Upsilon_k \tag{18a}$$

where Φ_k and Υ_k are made by taking portions of the exponential matrix of the following A matrix.

$$A = \begin{bmatrix} -F & GQG^T \\ 0 & F^T \end{bmatrix}\Delta t \tag{18b}$$

with F, G, and Q defined as

$$F = \begin{bmatrix} -\left[\hat{\omega}_{d/I}^d\times\right] & 0_{3\times3} & -I_{3\times3} & 0_{3\times3} & 0_{3\times9} - A_H^d(\hat{q}_{d/H})n \\ 0_{3\times3} & -\left[\hat{\omega}_{c/I}^c\times\right] & 0_{3\times3} & -I_{3\times3} & 0_{3\times9} - A_H^c(\hat{q}_{c/H})n \\ 0_{3\times3} & 0_{3\times3} & 0_{3\times3} & 0_{3\times3} & 0_{3\times10} \\ 0_{3\times3} & 0_{3\times3} & 0_{3\times3} & 0_{3\times3} & 0_{3\times10} \\ 0_{10\times3} & 0_{10\times3} & 0_{10\times3} & 0_{10\times3} & \frac{\partial f(X)}{\partial X}|_{\hat{X}} \end{bmatrix} \tag{18c}$$

where $\frac{\partial f(X)}{\partial X}|_{\hat{X}}$ is the partial derivative of the nonlinear state space models of Equations (5).

$$G = \begin{bmatrix} -I_{3\times3} & 0_{3\times3} & 0_{3\times3} & 0_{3\times3} & 0_{3\times3} \\ 0_{3\times3} & -I_{3\times3} & 0_{3\times3} & 0_{3\times3} & 0_{3\times3} \\ 0_{3\times3} & 0_{3\times3} & I_{3\times3} & 0_{3\times3} & 0_{3\times3} \\ 0_{3\times3} & 0_{3\times3} & 0_{3\times3} & I_{3\times3} & 0_{3\times3} \\ 0_{3\times3} & 0_{3\times3} & 0_{3\times3} & 0_{3\times3} & 0_{3\times3} \\ 0_{3\times3} & 0_{3\times3} & 0_{3\times3} & 0_{3\times3} & I_{3\times3} \\ 0_{4\times3} & 0_{4\times3} & 0_{4\times3} & 0_{4\times3} & 0_{4\times3} \end{bmatrix} \tag{18d}$$

$$Q = \begin{bmatrix} \sigma_{d\nu}^2 I_{3\times3} & 0_{3\times3} & 0_{3\times3} & 0_{3\times3} & 0_{3\times3} \\ 0_{3\times3} & \sigma_{c\nu}^2 I_{3\times3} & 0_{3\times3} & 0_{3\times3} & 0_{3\times3} \\ 0_{3\times3} & 0_{3\times3} & \sigma_{du}^2 I_{3\times3} & 0_{3\times3} & 0_{3\times3} \\ 0_{3\times3} & 0_{3\times3} & 0_{3\times3} & \sigma_{cu}^2 I_{3\times3} & 0_{3\times3} \\ 0_{3\times3} & 0_{3\times3} & 0_{3\times3} & 0_{3\times3} & \sigma_{\omega}^2 \end{bmatrix} \tag{18e}$$

where the σ values are variances of the process noise. Taking the matrix exponential of A, the Φ and Υ can be found.

$$B = e^A = \begin{bmatrix} B_{11} & B_{12} \\ 0 & B_{22} \end{bmatrix} = \begin{bmatrix} B_{11} & \Phi^{-1}\Upsilon \\ 0 & \Phi^T \end{bmatrix} \tag{19}$$

$$\Phi = B_{22}^T$$

$$\Upsilon = \Phi B_{12}$$

With these propagation steps, the EKF will accurately predict the true states to a degree specified by the state covariance matrix. This will include an estimate of the relative quaternions, the relative position in the Hill Frame, the relative rate of change of the position, the drift of the gyros of each satellite, the radius and rate of change of the radius of the RSO orbit, and the true anomaly and rate of change of the true anomaly of the RSO orbit. Of course, the EKF must be adjusted to fit the scenario of this specific project. Firstly, the RSO will not be giving gyro measurements; rather a controller in the filter will be determining the assumed maneuvers, which will lead into the MMAE discussed in the next chapter. The EKF also does not estimate the quaternion of the RSO alone, rather it estimates the relative quaternion between the RSO and the OS, and will produce the probability vector of the different pointing modes. The overview of the filter presented in this report is not meant to be exhaustive; more thorough derivations and discussions of the filter can be found in [3] and [4].

5.0 MULTIPLE MODEL ADAPTIVE ESTIMATION

5.1 MMAE Structure

The Multiple Model Adaptive Estimator (MMAE) holds a bank of EKFs, each of which uses a different control law. The different control laws are implemented to follow a respective pointing mode, so in that sense each EKF is assigned to a specific pointing mode. The output from each EKF goes into the MMAE, and the MMAE calculates the probability that each EKF holds the correct model. An in depth discussion of MMAE algorithms can be found in [1], and a summary is shown here.

Each EKF outputs a new estimate, covariance, residual, and residual covariance matrix based on the assumed mode setting and propagation and update relations. The estimator uses an Interacting Multiple Model (IMM) algorithm to combine the estimates and covariances back into unison to be put back into the EKFs for the following iteration. In order to do this, the probability that each mode is the true mode must be calculated. Coincidentally, this is also the intended output of the estimator in this case. The mode probability is solved for using a likelihood function and a mode transitioning matrix. The likelihood function is a function of the residual and its covariance at the jth EKF, where j runs through the number of EKFs, M. The residual covariance, E, was calculated in the update stage of the EKF as part of the Kalman Gain.

$$E^{-(j)} = H^{(j)} P^{-(j)} H^{(j)T} + R^{(j)} \tag{20}$$

$$L = p\left(\tilde{y}^{-(j)}\right) = \frac{1}{[det(2\pi E^{-(j)})]^{\frac{1}{2}}} e^{-\frac{1}{2}\nu^{-(j)T}(E^{-(j)})^{-1}\nu^{-(j)}} \tag{21}$$

The mode transitioning matrix is a probability density function detailing the time-varying mode sequence as a Markov process for M modes. The diagonal elements are the probability that the mode does not change on an iteration, which is close to 1 because there are thousands of iterations and the mode only changes a few to several times. The off diagonal elements are the probability that the mode changes to the corresponding mode of that element, which is the same probability between all off-diagonal elements.

$$\Pi_M = \begin{bmatrix} \pi_1 & \pi_2 & \cdots & \pi_2 \\ \pi_2 & \pi_1 & \cdots & \pi_2 \\ \vdots & \vdots & \ddots & \vdots \\ \pi_2 & \pi_2 & \cdots & \pi_1 \end{bmatrix} \to 1 \approx \pi_1 < 1, \pi_2 = \frac{1 - \pi_1}{M - 1} \tag{22}$$

With the likelihood function and the mode transitioning matrix, the mode probability, μ, is calculated and normalized below. Notice that the mode probability is directly related

to the mode probability of the previous iteration. For the first iteration, the initial mode probability used makes each mode equally likely, so $\mu_0^{(j)} = \frac{1}{M}$

$$\mu_k^{(j)} = \mu_{k-1}^{(j)} p(\tilde{y}^{-(j)}) \tag{23}$$

$$\mu_k^{(j)} = \frac{\mu_k^{(j)}}{\sum_{j=1}^{M} \mu_k^{(j)}} \tag{24}$$

$$\mu_k = \begin{bmatrix} \mu_k^{(1)} & \mu_k^{(2)} & \cdots & \mu_k^{(M)} \end{bmatrix} \tag{25}$$

Equation (25) is the mode probability vector of the different EKFs, corresponding directly to the probability of the correct RSO controller, however more steps are needed to allow the estimator to continue in the following iterations. There are still M estimates and covariances, and these need to be combined in a probabilistic manner in order to be useful, which will be done in a reinitialization step.

5.2   MMAE - Reinitialization

The reinitialization step of the estimator takes the estimates and covariances from each of the EKFs and intelligently recombines them for the next iteration through the use of a mixing probability. [1] The mixing probability is a function of the mode transitioning matrix and the current mode probability, essentially showing the probability of each mode in the upcoming iteration.

$$\mu_k^{(i|j)} = \frac{\mu_k^{(i)} \Pi_{ij}}{\sum_{i=1}^{M} \mu_k^{(i)} \Pi_{ij}} \tag{26}$$

Where the probability of each EKF, columns of i, being the EKF used in the next iteration given the EKF, rows of j, used to find the estimate being evaluated. In a typical IMM algorithm, the estimates are combined with a simple relationship:

$$\hat{x}_k^{+0(j)} = \sum_{i=1}^{M} \mu_k^{(i|j)} \hat{x}_k^{+(i)} \tag{27}$$

Due to the nature of quaternions, they cannot be directly averaged using a weighting matrix and must differ from the standard MMAE algorithms for this reason. A method that can be used to find the average quaternion is found in. [5] This is only the case for the quaternion part of the estimate, and the angular rate still uses the relationship shown above.

$$W = \sum_{i=1}^{M} \mu_k^{(i|j)} \hat{x}_k^{+(i)} \tag{28}$$

$$\hat{x}_k^{+0(1:4)} = MaxEigVec(W) \tag{29}$$

In the quaternion averaging algorithm, the averaged quaternion will be the eigenvector corresponding to the maximum eigenvalue given by matrix W. The complete vector of the

combined estimate comes simply from merging the combined quaternion and angular rate estimates.

$$\hat{x}_k^{+0} = \begin{bmatrix} \hat{x}_k^{+0(1:4)} \\ \sum_{i=1}^M \mu_k^{(i|5:7)} \hat{x}_{k,5:7}^{+(i)} \end{bmatrix} \tag{30}$$

The covariance also needs to be combined in a probabilistic manner similar to the estimate. In a typical IMM structure, this would look like the following

$$P_k^{+0(j)} = \sum_{i=1}^M \mu_k^{(i)} \left[P_k^{+(i)} + (\hat{x}_k^{+(i)} - \hat{x}_k^{+0(j)})(\hat{x}_k^{+(i)} - \hat{x}_k^{+0(j)})^T \right] \tag{31}$$

Once again, the multiplicative nature of quaternions becomes problematic in an algorithm that is designed to combine terms additively, and the covariance is of the error state in the estimator. The quaternion part of the estimate in the covariance mixing is replaced with error angles, which are solved for by approximating them to be roughly four times the error modified Rodrigues parameters, where the quaternion error state is found multiplicatively from the measurement of a given EKF and the mixed quaternion estimate.

$$\delta q = \hat{x}_k^{+0(1:4)} \otimes \hat{x}_{1:4}^{(i)-1} \tag{32}$$

$$\delta\theta \approx 4\delta p = \frac{4\delta q_{1:3}}{1 + \delta q_4} \tag{33}$$

The angular rate will be able to use the straight subtraction that is used in a typical IMM algorithm. The estimate error state, including both the error angles and the error angular rate, can then be combined into one vector to be used in Equation (31).

$$\delta x = \begin{bmatrix} \delta\theta \\ \hat{x}_k^{+0(5:7)} - \hat{x}_{5:7}^{(i)} \end{bmatrix} \tag{34}$$

$$P_k^{+0(j)} = \sum_{i=1}^M \mu_k^{(i)} \left[P_k^{+(i)} + \delta x \delta x^T \right] \tag{35}$$

The combined estimate and covariance will be the input to each EKF for the next time step, and in this way the loop is completed and mode probabilities will continue to be calculated for each incoming measurement.

6.0 RESULTS

6.1 Filter

The simulation of the relative dynamics between the RSO was run with a time span of three days, equivalent to three full orbits of both satellites. Before the MMAE was added to the estimator, the EKF was developed and tested. An example of a result of the states of the relative quaternions, relative distances, and RSO radius and true anomaly are shown in Figures 3 - 7 where state errors are plotted with their 6σ bounds.
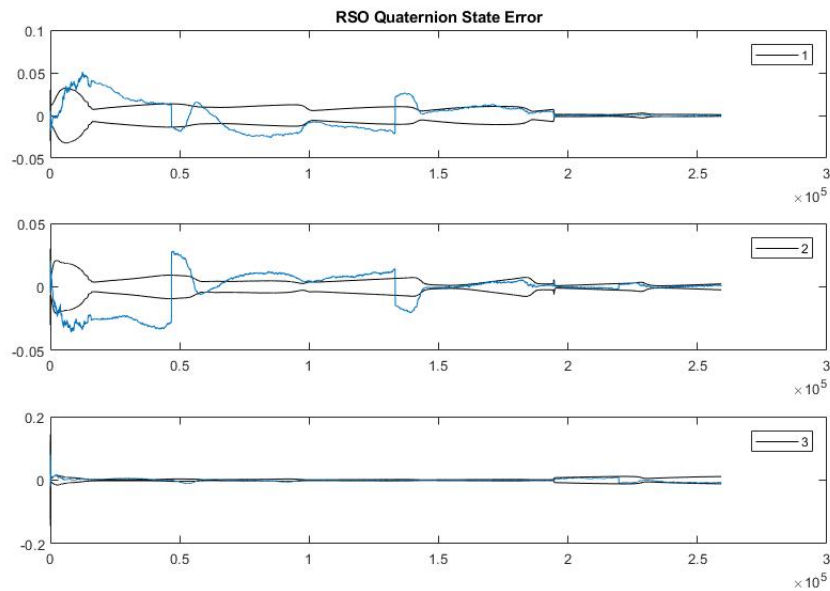
Figure 3: State Error of Relative Quaternion Between RSO and Hill Frame

As is shown, the states do not converge within the covariance bounds immediately upon starting the filter, but they do converge given time. Once the states converge, they do not break outside of the bounds away from the truth. This could cause problems for the MMAE, because it will be relying on a filter that is able to completely converge within the covariance bounds quickly. The simultations shown in this report are done using the filter with the shown results. One way to improve performance of the MMAE could be to wait until the filter is converged, and then input the MMAE to begin tracking the mode probability. Another possible solution is to weight the likelihood of some filters over others,
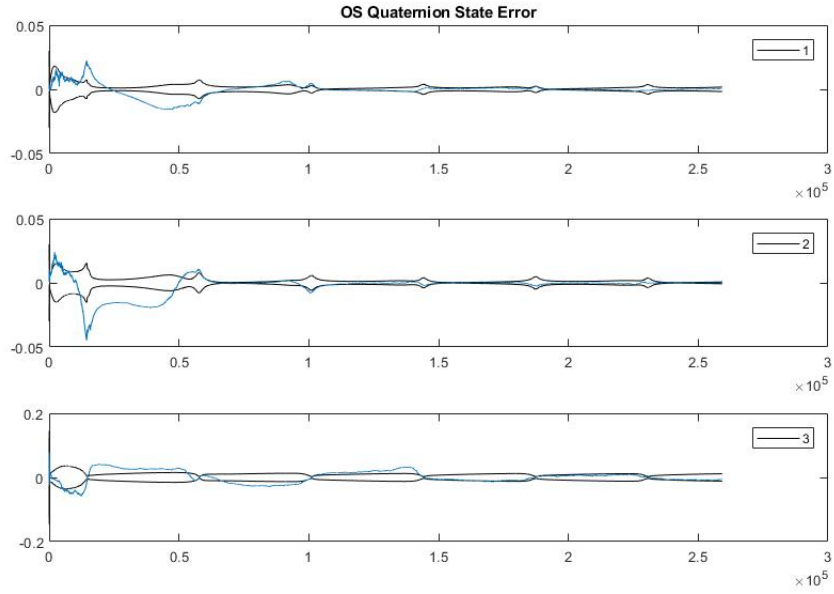
Figure 4: State Error of Relative Quaternion Between OS and Hill Frame
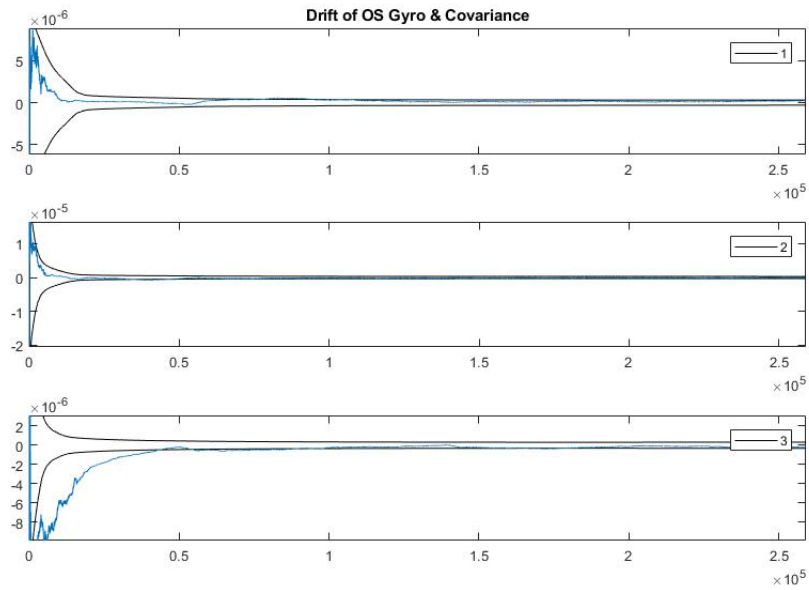
Figure 5: State Error of the Drift of the OS Gyro

because the filter itself acts better with some RSO controllers over others. Weighting the likelihood function in the MMAE could help to negate these patterns. Once the MMMAE is added in, which will be shown in the following results, the filter has a much more difficult time converging. This could lead to errors in the mode detection results.
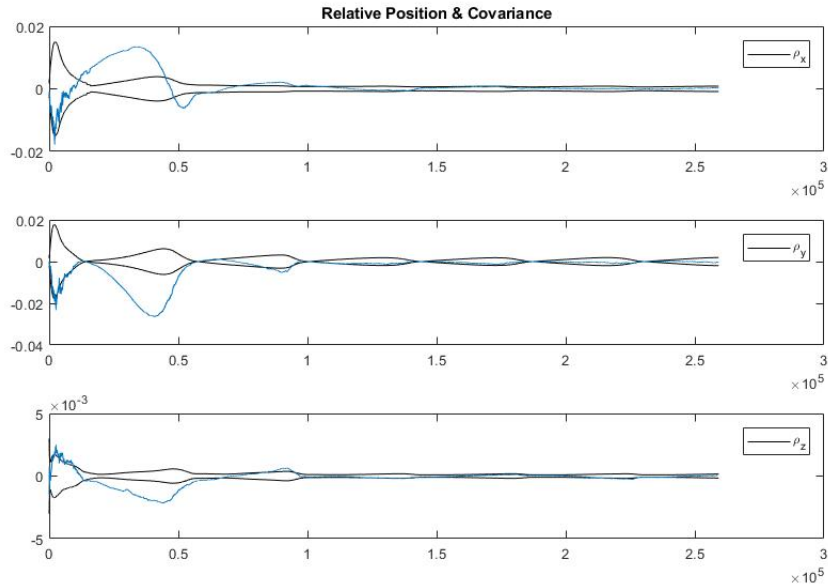
Figure 6: State Error of the Relative Positions
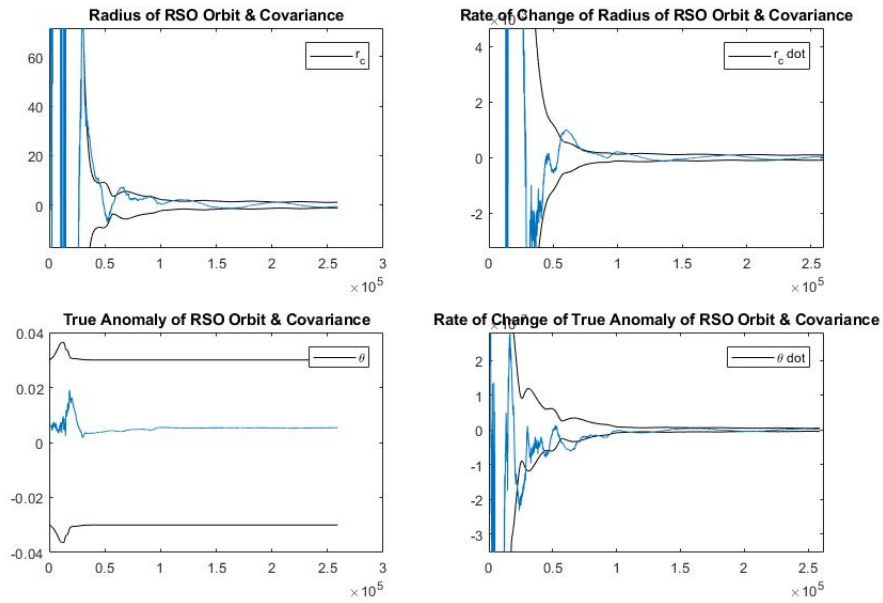
Figure 7: State Error of the RSO Radius and True Anomaly

6.2 Mode Estimation

First, results are shown with using the standard filter and MMAE as descibed throughout the report. Figure 8 indicates the mode probabilities throughout the simulation, using the mode scheudle shown in Table 1.
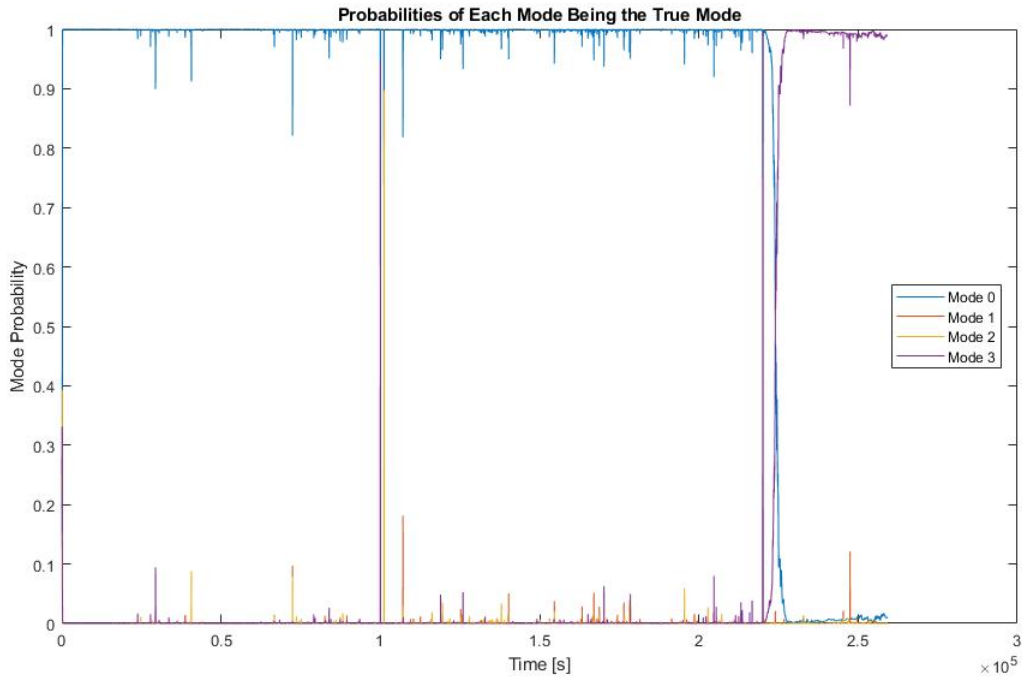
Figure 8: Mode Probabilities With Standard EKF and MMAE. Mode 1 is Sun Pointing, Mode 2 is Earth Pointing, Mode 3 is Inertial Pointing, and Mode 0 is Uncontrolled Tumble

Clearly, a filter which takes a long time to converge has an effect on the mode estimator. While the filter is converging, the MMAE has a difficult time estimating the correct EKF, because none of them are showing the true value. When this occurs, an uncontrolled tumble appears to be more likely than the other controllers. Towards the end of the simulation, the filter is much closer to converging behind the scenes, and the estimator can more accurately estimate the true mode of the RSO. This is why the estimator correctly changes the predicted mode from mode 0 to mode 3. Figure 9 shows one of the states in this example to demonstrate the level of convergence of the filter while the MMAE is active.

With the MMAE active, the relative position state does not fully converge to within the covariance bounds, however it greatly improves throughout the simulation. This trend is followed by each of the remaining states in the filter as well. To reiterate, in the beginning when the states are far from being converged, the MMAE is not able to correctly estimate the mode of the RSO controller. Once the states get closer to their true values, the MMAE performs as intended.

One way to adjust the MMAE to act favorably is by weighting the likelihood function to account for the modes that are viewed favorably by the estimator while the filter has yet to converge. For example, before the filter converges the MMAE is more likely to predict an Uncontrolled tumble as being the correct mode, regardless of which mode the RSO is truly set to. By reducing the weight of the uncontrolled tumble in the likelihood function, the other modes are allowed to be seen more favorably upon the estimator. Figure 10 demonstrates the effect that weighting the likelihood function can have on the mode estimator.
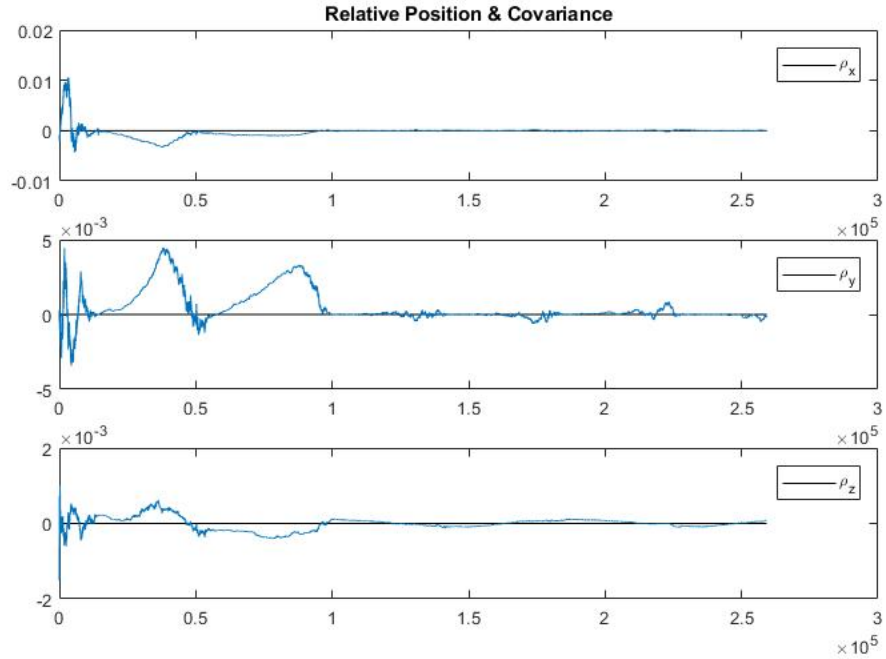
Figure 9: Relative Position State Error and Covariance With MMAE Active

As Figure 10 shows, the MMAE still does not perform perfectly, but it is much improved. The beginning of the simulation accurately predicts Sun Pointing as the correct mode, and the end of the simulation accurately predicts Inertial Pointing. The MMAE still has trouble discerning between Earth Pointing and an uncontrolled tumble, but this is still with the filter acting in the same way as Figure 9.
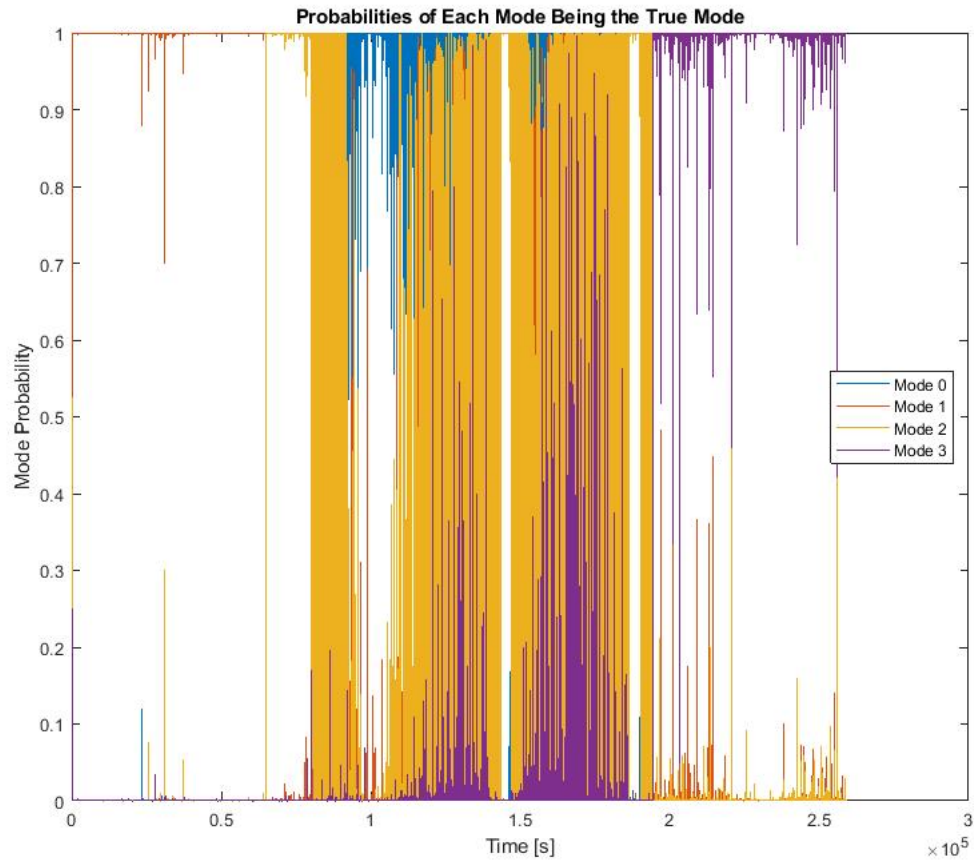
Figure 10: Mode Probabilities With a Weighted Likelihood Function in the MMAE. Mode 1 is Sun Pointing, Mode 2 is Earth Pointing, Mode 3 is Inertial Pointing, and Mode 0 is Uncontrolled Tumble

7.0 FUTURE WORK

The mode estimator continues to have room for improvement. The MMAE algorithm seems to be working for a converged filter, however the performance of the filter is imperative for the success of the MMAE. Since it takes so long for the filter to converge, the MMAE struggles to work as intended. Moving forward, more time should be invested in the convergence of the filter, particularly upon initiation of the algorithm. If the filter can converge immediately, the mode estimation will be accurate.

8.0 REFERENCES

[1] Crassidis, J. L. and Junkins, J. L., *Optimal Estimation of Dynamic Systems*, CRC Press, Boca Raton, FL, 2012.

[2] Schaub, H. and Junkins, J. L., *Analytical Mechanics of Aerospace Systems*, American Institute of Aeronautics and Astronautics, Reston, VA, 2003.

[3] Zhang, L., Yang, H., Zhang, S., Cai, H., and Qian, S., "Kalman Filtering for Relative Spacecraft Attitude and Position Estimation: A Revisit," *Journal of Guidance, Control, and Dynamics*, **Vol. 37**, No. 5, Sept.-Oct. 2014, pp. 1706–1711.

[4] Kim, S., Crassidis, J. L., Cheng, Y., and Fosbury, A., "Kalman Filtering for Relative Spacecraft Attitude and Position Estimation," *Journal of Guidance, Control, and Dynamics*, **Vol. 30**, No. 1, Jan.-Feb. 2007, pp. 133–143.

[5] Markley, F. L., Cheng, Y., Crassidis, J. L., and Oshman, Y., "Averaging Quaternions," *Journal of Guidance, Control, and Dynamics*, **Vol. 30**, No. 4, July-Aug. 2007, pp. 1193–1197.

[6] Clohessy, W. and Wiltshire, R., "Terminal Guidance System for Satellite Rendezvous," *Journal of the Aerospace Sciences*, **Vol. 27**, No. 9, pp. 653–658.

[7] Inalhan, G., Tillerson, M., and How, J. P., "Relative Dynamics and Control of Spacecraft Formations in Eccentric Orbits," *Journal of Guidance, Control, and Dynamics*, **Vol. 25**, No. 1, Jan.-Feb. 2002, pp. 48–59.

DISTRIBUTION LIST

DTIC/OCP
8725 John J. Kingman Rd, Suite
0944 Ft Belvoir, VA 22060-6218   1 cy

AFRL/RVIL
Kirtland AFB, NM 87117-5776   1 cy

Official Record Copy
 AFRL/RVS/Thomas Lovell   1 cy